

Calcium Carbonate Precipitation Kinetics, Part 2 Effects of Magnesium

BENJAMIN, L, LOEWENTHAL, R E and G v R MARAIS
[DEPARTMENT OF CIVIL ENGINEERING, UNIVERSITY OF CAPE TOWN,
RONDEBOSCH 7700, CAPE TOWN]

Abstract

The precipitation kinetics of CaCO_3 in the presence of Mg^{++} can be formulated in terms of the hypothesis of Davies and Jones for calcite seeded solutions:

$$-\delta[\text{Ca}_T]/\delta t = \text{KM}f_D^2[\text{Ca}^{++}]^{\frac{1}{2}}[\text{CO}_3^{\equiv}]^{\frac{1}{2}} - (\text{K}_{spa}/f_D^2)^{\frac{1}{2}}^2$$

where

K_{spa} = an apparent molar solubility product for CaCO_3

K = the precipitation rate constant for magnesian calcite $(\text{min (moles}/\ell)^2)^{-1}$.

The apparent solubility product, K_{spa} , is related to the solubility product for magnesian calcite, K_{spm} , as follows:

$$\text{K}_{spa} = \frac{\text{K}_{spm}}{((\text{Mg}^{++})/(\text{Ca}^{++}))^x}$$

where

x = mole fraction of MgCO_3 in the magnesian calcite.

Both the solubility product for magnesian calcite, K_{spm} , and the precipitation rate constant, K , vary with the ratio of magnesium to calcium in the aqueous solution:

$$\text{pK}_{spm} = 8,40 - 0,0349 \{(\text{Mg}^{++})/(\text{Ca}^{++})\}$$

$$\text{K} = \text{K}_o^{-0,566} (\text{Mg}^{++})/(\text{Ca}^{++})$$

where

K_o = the precipitation rate constant for pure calcite $(\text{min(moles}/\ell)^2)^{-1}$.

Introduction

Sturrock, Benjamin, Loewenthal and Marais (1976) proposed Eq. (1) as a model for the kinetics of CaCO_3 precipitation from

water containing only sodium, chloride, calcium, carbonic species and calcite seed crystals:

$$-\delta[\text{Ca}_T]/\delta t = \text{KM}f_D^2[\text{Ca}^{++}]^{\frac{1}{2}}[\text{CO}_3^{\equiv}]^{\frac{1}{2}} - (\text{K}_{sp}^2/f_D)^{\frac{1}{2}}^2 \quad (1)$$

where

K = rate constant of precipitation $(\text{min(moles}/\ell)^2)^{-1}$

M = mass of seed (moles/ ℓ)

$[\text{Ca}_T]$ = molar mass of dissolved calcium*

K_{sp} = thermodynamic solubility product for CaCO_3 in the molar form

f_D = activity coefficient for a divalent ion.

This equation is based on the hypothesis that a charge is set up on the crystal seed such that there are equal concentrations of Ca^{++} and CO_3^{\equiv} in the monolayer surrounding the crystal. It was shown experimentally that Eq. (1) held for a range of conditions, for example, initial pH, initial supersaturation and initial seed mass (see Part 1, Sturrock *et al* (1976)).

In practice however, many other anionic and cationic species will be present in natural waters and these ions may interfere with precipitation of Ca^{++} and CO_3^{\equiv} ions from the monolayer onto the crystal seed. In this report the effect of Mg^{++} ions on the kinetics of CaCO_3 precipitation is investigated.

Hypotheses

In calcium water softening the presence of Mg^{++} ions apparently causes both incomplete and slow CaCO_3 removal. Three possible explanations to these observations are:

*In this paper round brackets, i.e. (Ca^{++}) signify active concentrations; square brackets, i.e. $[\text{Ca}^{++}]$, signify molar concentrations; no brackets, i.e. Ca^{++} , signify concentrations in ppm expressed as CaCO_3 . Square brackets with subscript T signify the total dissolved molar species concentration, i.e. free plus ion paired species.

Ion pair formation

Formation of MgCO_3° ion pairs reduces the free CO_3^{2-} in the solution and hence reduces the CaCO_3 supersaturation below that apparent value calculated ignoring MgCO_3° ion pairing effects. The CaCO_3 crystallization rate and the final CaCO_3 saturated Ca^{++} value are then affected by the reduced free CO_3^{2-} concentration. However, in doing particular softening calculations where ion pairing effects have been duly allowed for in the equilibrium chemistry calculations, there is still a significant disparity between the observed and calculated rates of Ca^{++} removal and final equilibrium values.

Crystal poisoning (Stumm and Morgan, 1972; and Berner, 1974)

Mg^{++} ions may cause poisoning of the CaCO_3 seed crystal. Since the rate determining step is at the interface, small amounts of foreign constituents may retard crystallization by obstructing growth sites. Davies and Nancollas (1955) have shown that in the precipitation of AgCl from seeded solutions, the rate constant for crystal growth is reduced by an amount reflecting the extent of adsorption of foreign constituents.

Nature of precipitate

If CaCO_3 precipitates from an aqueous solution in the presence of Mg^{++} , MgCO_3 may be incorporated into the crystal lattice of the precipitant. If this is correct, it is to be expected that both the solubility of the precipitant and the rate constant for precipitation will change.

In this investigation research was orientated towards testing the third hypothesis.

Basic Considerations

Calcium carbonate may precipitate from water in one (or more) of three forms: calcite, aragonite and vaterite. Which of these allotropes precipitate depends on pressure and temperature conditions, the rate at which precipitation occurs (Roques and Girou, 1974), the nature and mass of crystal seed and/or the presence of foreign ions.

Foreign ions may be incorporated into a precipitate provided that these can fit into the crystal lattice (Krauskopf, 1967). Many investigators have shown that magnesian calcite (i.e. calcite containing MgCO_3) may be formed when calcite precipitates in the presence of Mg^{++} . The fraction of MgCO_3 in the crystal varies between magnesian calcites and depends primarily on the ratio of $\text{Mg}^{++}/\text{Ca}^{++}$ in the aqueous phase (Winland, 1969).

Magnesian calcites may exist in aqueous solutions either as a thermodynamically stable solid phase of a meta-stable phase, (Pytkowicz, 1965; Berner, 1974) or as a non equilibrium steady state solid phase, (Chave, Deffeyes, Weyl, Garrels and Thompson, 1962), the last two being transient phases. The time required for stable thermodynamic equilibrium to be attained from a transient solid phase is generally in terms of geological time. In water softening the time of residence of the seed (sludge) is relatively short. Hence crystal changes after the

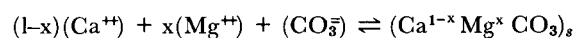
solid has precipitated, to attain equilibrium with respect to the solid phase, are unlikely to be significant.

The allotropes of CaCO_3 and the various magnesian calcites differ in mineral structure and thus in solubility. Whereas the solubility product for the allotropes calcite and aragonite have been firmly established, (Helgeson, 1969), no firm values have been established to date for the magnesian calcites. This probably stems from difficulties associated with solubility measurement of these calcites.

Solubility measurements usually are carried out by means of either precipitation or dissolution experiments utilizing batch tests. In precipitation experiments the solution must be seeded with calcite or magnesian calcite crystals. As precipitation proceeds the $(\text{Mg}^{++})/(\text{Ca}^{++})$ ratio changes in the bulk solution resulting in the formation of crystal layers of differing composition. Consequently the crystal varies in composition from the surface inwards making it extremely difficult to determine the crystal composition corresponding to a particular $(\text{Mg}^{++})/(\text{Ca}^{++})$ ratio in the aqueous phase.

In dissolution experiments magnesian calcites formed in life process (i.e. the carbonate skeletal materials of marine organisms) are used (Chave *et al.*, 1962; Plummer and Mackenzie, 1974). These carbonates have the merit that the crystal constitution is relatively homogeneous, i.e. the ratio of magnesium to calcium in the lattice is constant. However, dissolution experiments present the problem of incongruent precipitation coexisting with the dissolution process, that is, the magnesian calcite dissolves and either aragonite or pure calcite or a different magnesian calcite precipitates. This behaviour results in a steady state situation being established (i.e. a condition of non equilibrium) between the dissolving and precipitating minerals.

Chave *et al.* (1962) reported steady state pH values attained in batch dissolution experiments on magnesian calcites of known composition in distilled water at a partial pressure of $P_{\text{CO}_2} = 1$ atmosphere and temperature 25°C . In order to obtain solubility products from Chave *et al.*'s data, Winland (1969) postulated that for a solution in stable or meta stable equilibrium with respect to a magnesian calcite, a dynamic state exists between the solid phase and Mg^{++} , Ca^{++} and carbonic species in the aqueous phase which he formulates as:



i.e.

$$(\text{Ca}^{++})^{1-x}(\text{Mg}^{++})^x(\text{CO}_3^{2-}) = K_{spm} \quad (2)$$

where

K_{spm} = the solubility product for magnesian calcite, which varies with x

x = the mole fraction of MgCO_3 in the lattice, i.e.

$$x = \frac{(\text{MgCO}_3)_s}{[(\text{CaCO}_3)_s + (\text{MgCO}_3)_s]} = \frac{(\text{Mg})_s}{[(\text{Ca})_s + (\text{Mg})_s]} \quad (3)$$

Subscript 's' denotes solid species.

Using the data of Chave *et al.*, Winland calculated the solubility product values for K_{spm} versus X (Table 1). Similar calculations on Chave *et al.*'s data made by Plummer and Mackenzie (1974) and by ourselves, are also listed in Table 1.

TABLE 1
COMPARISON OF SOLUBILITY PRODUCTS,
pK_{spm}, FOR VARIOUS MAGNESIAN
CALCITES AT 25°C AND TOTAL
ATMOSPHERIC PRESSURE.

Mole fraction MgCO ₃ in magnesian calcite	Data from Chave <i>et al</i> ¹ calculated by			Data from	Data ⁵ used in this paper
	Winland ²	Plummer & ³ Mackenzie	This paper	Plummer & ⁴ Mackenzie	
0	8,35	8,35	8,35	8,49	8,40
0,50	8,22	8,45	8,35	8,35	8,31
0,10	8,02	8,40	8,25	8,00	8,23
0,15	7,84	8,15	8,08	7,70	8,14

1. Chave *et al* (1962)
2. Winland (1969)
- 3 and 4 Plummer and Mackenzie (1974)
5. Interpolated from the values reported by 3 and 4 above (see Fig. 1)

Whereas Plummer and Mackenzie's and our values correspond closely, those of Winland show discrepancy. The reason for this difference is not clear. Perhaps Winland did not use free ion species concentrations, but even if K_{spm} values are recalculated using total ion species concentrations his values are still significantly different.

When Chave *et al* reported their results they stated that the data were not necessarily obtained from congruent precipitation and hence would probably give rise to minimum solubilities (i.e. maximum pK_{spm} values). Plummer and Mackenzie performed similar batch dissolution experiments to those of Chave *et al* but attempted to identify the congruent phase of dissolution by monitoring the pH changes throughout the experimental period. By examination of the pH time plot they state they were able to identify the congruent phase and by extrapolating these phase data to time infinity they estimated the solubility products using Eq. (2) (see Table 1). They state that their procedures possibly give rise to maximum solubility values (i.e. minimum pK_{spm} values). Hence the true pK_{spm} values probably lie between the maximum values calculated from Chave *et al*'s data and the minimum values of Plummer and Mackenzie.

The data plotted in Fig. 1 for calcite and magnesian calcite solubility indicate the wide variability between values reported. Nevertheless, the data do show the distinct trend of decrease in pK_{spm} with increase in mole fraction of MgCO₃ in the solid. In general the pK_{spm} values reported by Plummer and Mackenzie are lower than those calculated from Chave *et al* which is consistent with their respective experimental procedures as discussed above. However, the pK value for calcite measured by Plummer and Mackenzie (i.e. pK(calcite) = 8,49 assuming pK(CaHCO₃) = 1,31) is exceptionally *high* compared with the generally accepted value reported by Helgeson (1969), i.e. pK(Calcite) = 8,40 at 25°C. We can offer no explanation for this apparent inconsistency.

In this paper, the data used for equilibrium constants are those reported by Helgeson. Solubility products for the magne-

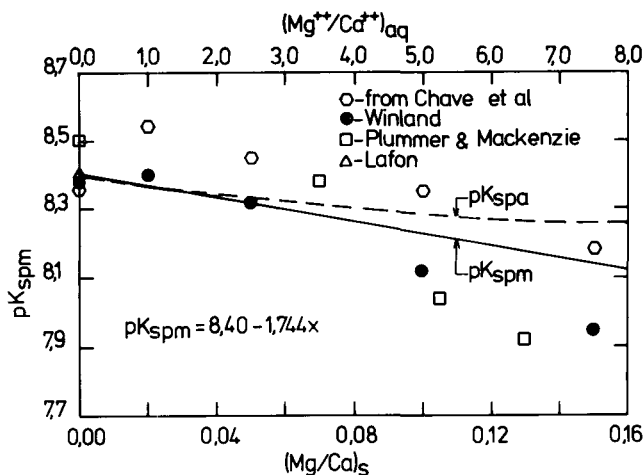


Figure 1
Dependence of magnesian calcite solubility product on the (Mg⁺⁺)/(Ca⁺⁺)
ratio

sian calcite were obtained by linear interpolation from the data shown in Fig. 1, using the data of Plummer and Mackenzie (1974) and Chave *et al* (1962) as interpolated by Plummer and Mackenzie (1974).

$$pK_{spm} = 8,40 - 1,744x \quad (4)$$

where

x is the mole fraction of MgCO₃ in the magnesian calcite lattice.

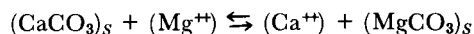
The form in which Eq. (4) is expressed is inconvenient when inserted into Eq. (1). Eq. (4) can be transformed to be in terms of (Ca⁺⁺) and (CO₃⁼) formulating the solubility product as an apparent one

$$(Ca^{++})(CO_3^{=}) = \frac{K_{spm}}{\{(Mg^{++})/(Ca^{++})\}^x} = K_{spa} \quad (5)$$

where

K_{spa} = the apparent CaCO₃ solubility product.

An estimate of x in Eq. (5) can be made by considering isomorphism and partitioning phenomena (Krauskopf, 1967): since Mg⁺⁺ can fit into the calcite crystal structure, when calcite is precipitated from a solution containing Mg⁺⁺ ions, the Mg⁺⁺ ions distribute themselves between the solid and aqueous phase, Winland (1969),



thus for equilibrium, from the above reaction

$$\frac{(Ca^{++})(Mg)_s}{(Mg^{++})(Ca)_s} = D \quad (6)$$

where

D = an equilibrium constant also referred to as a distribution coefficient for partitioning.

This equation is reformulated below into the usual form of partitioning equations

$$(Mg)_s/(Ca)_s = D\{(Mg^{++})/(Ca^{++})\} \quad (7)$$

Winland has measured the distribution coefficient for partitioning of Mg^{++} between calcite and the aqueous phase by precipitating the $CaCO_3$ in the presence of Mg^{++} . He reported that for initial $(Mg^{++})/(Ca^{++})$ ratios from 0,025 to 5,3, $D = 0,02$. In Eq. (7) assuming Winland's observations are applicable to this investigation, x can be calculated:

From Eq. (3)

$$x = (Mg)_s / \{(Mg)_s + (Ca)_s\}$$

i.e.

$$x = 1 / \{1 + (Ca)_s / (Mg)_s\} \quad (8)$$

Incorporating the distribution coefficient from Eq. (7) with $D = 0,02$, into Eq. (8) and reducing:

$$x = 1 / \{1 + 50 (Ca^{++}) / (Mg^{++})\} \quad (9)$$

that is, the fraction of $MgCO_3$ in the crystal depends only on the ratio of (Mg^{++}) to (Ca^{++}) in the aqueous phase.

Knowing x , and hence K_{spm} , (from Eq. (4)) it is thus possible to calculate K_{spa} from Eq. (5). The corresponding pK_{spa} values calculated are plotted versus x and $(Mg^{++})/(Ca^{++})$ ratio in Fig. 1.

The precipitation model developed in Part 1 considered only the presence of the calcium and carbonic species in solution. The model *per se* need not necessarily describe the precipitation of magnesian calcites correctly. For this reason the model is redeveloped under slightly more general conditions.

Saturated conditions

Consider a seeded aqueous solution containing calcium, magnesium and carbonic species and just saturated with respect to magnesian calcite. As outlined in Part 1 a potential ψ is set up between an adsorbed layer of ions surrounding the crystal and the bulk solution. The value of ψ is such that equal concentrations of Ca^{++} and CO_3^{--} occur in this adsorbed layer, i.e.

$$\text{Concentration of } Ca^{++} \text{ in the monolayer} = (Ca^{++})_e^{-2\psi/RT} \quad (10)$$

$$\text{Concentration of } CO_3 \text{ in the monolayer} = (CO_3^{--})_e^{+2\psi/RT} \quad (11)$$

Considering that the solubility product established is that for $CaCO_3$ precipitation, from Eq. (5)

$$(Ca^{++})(CO_3^{--}) = \frac{K_{spm}}{(Mg^{++})/(Ca^{++})^x} = K_{spa} \quad (12)$$

where

K_{spa} is an apparent solubility product for $CaCO_3$ precipitation.

Thus, from Eq. (12), in the monolayer for saturation

$$\{(Ca^{++})_e^{-2\psi/RT}\} \{(CO_3^{--})_e^{+2\psi/RT}\} = K_{spa} \quad (13)$$

and from the initial assumption regarding equal concentrations of calcium and carbonate in the monolayer

$$(Ca^{++})_e^{-2\psi/RT} = (CO_3^{--})_e^{+2\psi/RT} = K_{spa}^{1/2} \quad (14)$$

Note that the $(Mg^{++})/(Ca^{++})$ ratio in the monolayer is equal to that in the bulk solution because Mg^{++} and Ca^{++} have similar charges. The value for K_{spa} is thus established by the $(Mg^{++})/(Ca^{++})$ ratio in the bulk solution.

Supersaturated conditions

Consider an aqueous solution supersaturated with respect to $CaCO_3$. From Part 1, the rate of precipitation is proportional to the mass of crystal seed (representing the number of growth sites) and the concentrations of calcium and carbonate available for precipitation.

The concentrations of Ca^{++} and CO_3^{--} available for precipitation are determined as follows:

$$\text{Concentration of } Ca^{++} \text{ in the monolayer} = (Ca^{++})_e^{-2\psi/RT} \quad (15)$$

$$\text{Concentration of } CO_3^{--} \text{ in the monolayer} = (CO_3^{--})_e^{+2\psi/RT} \quad (16)$$

The concentrations of these ions available for precipitation are equal to their concentrations in the monolayer minus the concentrations required for saturation, see Eq. (14):

$$(Ca^{++}) \text{ available for precipitation} = \{(Ca^{++})_e^{-2\psi/RT} - K_{spa}^{1/2}\} \quad (17)$$

$$(CO_3^{--}) \text{ available for precipitation} = \{(CO_3^{--})_e^{+2\psi/RT} - K_{spa}^{1/2}\} \quad (18)$$

Because the concentrations of Ca^{++} and CO_3^{--} in the monolayer are equal, from Eqs. (15 and 16) solve for $e^{2\psi/RT}$, i.e.

$$e^{2\psi/RT} = \{(Ca^{++})/(CO_3^{--})\}^{1/2} \quad (19)$$

Substituting Eq. (19) into Eqs. (17 and 18) and simplifying:

$$(Ca^{++}) \text{ available for precipitation} = \{(Ca^{++})^{1/2}(CO_3^{--})^{1/2} - K_{spa}^{1/2}\} \\ = (CO_3^{--}) \text{ available for precipitation.}$$

Having this information, a rate equation for $CaCO_3$ precipitation can be developed by assuming the rate to depend on (i) the number of growth sites available for precipitation, M , and (ii) the concentration of $CaCO_3$ available for precipitation, (see Part 1) to give:

$$\frac{\delta[CaCO_3]}{\delta t} = \alpha M f_D^2 \{ [Ca^{++}]^{1/2} [CO_3^{--}]^{1/2} - (K_{spa}/f_D^2)^{1/2} \}^2 \\ = K M f_D^2 \{ [Ca^{++}]^{1/2} [CO_3^{--}]^{1/2} - (K_{spa}/f_D^2)^{1/2} \}^2 \quad (20)$$

Noting that $\delta[CaCO_3]/\delta t = \delta[Ca_T]/\delta t$, and rewriting concentrations as ppm expressed as $CaCO_3$:

$$\frac{\delta Ca_T^{++}}{\delta t} = K^c M f_D^2 \{ Ca^{++1/2} CO_3^{--1/2} - K_{spa}^{1/2}/f_D \}^2 \quad (21)$$

Where the superscript 'c' indicates that concentrations incorporated in the constant are in ppm expressed as $CaCO_3$.

Equation (20) differs from Eq. (1) in that K_{spa} replaces the solubility product for calcite, K_{sp} . The value of K_{spa} is greater than K_{sp} .

Calculations for determining the values of parameters in Eq. (21) requires the establishment of a model of the interactions of calcium, magnesium and the carbonate system in the aqueous

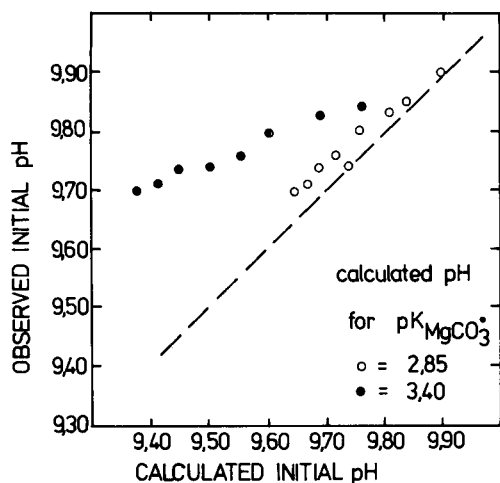


Figure 2
Correlation of calculated and observed initial pH for mixtures of Mg^{++} , Ca^{++} and carbonic species using two reported values for $pK_{MgCO_3^*}$

phase with magnesian calcite in the solid phase. One could use the model developed by Wiechers, Sturrock and Marais (1973) provided the pH remains below pH 10. Their model has the advantage that only one parameter, the pH, needs to be measured with time to enable all parameters to be calculated.

A more general approach, valid for any pH, is possible if the initial alkalinity is measured and pH is monitored throughout the experiment (Loewenthal and Marais, 1975). In order not to disrupt the continuity of the paper the basic theory for the calculation procedure is given in Appendix A. A computer printout for the calculation of the precipitation rates is set out by Benjamin, Loewenthal and Marais (1975).

Experimental Methods and Results

The method and apparatus for conducting the seeded batch precipitation tests were identical to those described by Wiechers *et al* (1973) except that in the $CaCl_2$ solution a magnesium/calcium ratio was established by adding $MgCl_2$.

In each experiment the initial condition of the water was controlled by varying the masses added of the reagent chemicals $CaCl_2$, $NaOH$, $NaHCO_3$ and $MgCl_2$. All the experiments were done at 20°C using calcite seed crystals from one batch of Merck (pro analysi) $CaCO_3$ at concentrations of 900, 1 500 and 2 000 ppm. The solutions were all made up using CO_2 free distilled water. A list of reagents added in each experiment and the pH time curves obtained are not reported here for lack of space, but are available in the report of Benjamin *et al* (1975).

Analysis and Discussion

Equilibrium constants

Implicit in the application of equilibrium chemistry to precipitation rate computations is that the values are known for the equilibrium constants of relevant equilibrium reactions. Values for all these constants have been firmly established excepting those for the ion pairs $MgCO_3^*$ and $MgHCO_3^*$. The K value for

$MgCO_3^*$ is particularly important because relatively high concentrations of this species can be expected in the pH range in which experiments were carried out (pH > 10).

There are two values available for $pK_{MgCO_3^*}$ at 20°C, that of Garrels and Christ (1965) ($pK_{MgCO_3^*} = 3,40$) and that interpolated from the values of Larsen, Sollo and McGurk (1973) ($pK_{MgCO_3^*} = 2,85$). These two values were tested by comparing the measured and theoretically predicted initial pH in a number of experiments in which ionic equilibrium had been established but precipitation had not yet commenced. The results are shown in Fig. 2. It is evident that using $pK_{MgCO_3^*} = 3,40$ gives rise to increasing divergence between the calculated and observed values as the initial (Mg^{++}) to (Ca^{++}) ratio increases, whereas using $pK_{MgCO_3^*} = 2,85$ gives close agreement between the theoretically predicted and observed initial pH values. It was concluded that $pK_{MgCO_3^*} = 2,85$ was the best available estimate for $pK_{MgCO_3^*}$. The $pK_{MgCO_3^*} = 2,85$ has been verified by work done in this laboratory (McLean, 1976).

Precipitation rate constant – pure systems

The rate constant for precipitation, K, varies both between different commercial brands of calcite and between batches of the same brand as pointed out by the authors in Part 1. This change in K reflects the variation in the surface area to mass between the various commercially supplied calcites.

In Part 1 the rate constant was determined for a single batch of Hopkins and Williams Analar brand calcite seed as $3,8 \times 10^{-5}$ (min (ppm as $CaCO_3$)²)⁻¹, i.e. $3,8 \times 10^5$ (min(moles/l)²)⁻¹. In this investigation one batch of calcite supplied by Merck was used throughout. Before proceeding with the investigation of the effects of magnesium on precipitation kinetics, the rate constant for this seed in pure systems was determined as $5,7 \times 10^{-5}$ (min(ppm as $CaCO_3$)²)⁻¹, i.e. $5,7 \times 10^5$ (min(moles/l)²)⁻¹.

CaCO₃ solubility

To verify if in these series of experiments there is evidence, as reported, that the solubility product changes when Mg^{++} is present, the rates of precipitation were calculated assuming K_{sp} remains constant at the values for pure calcite.

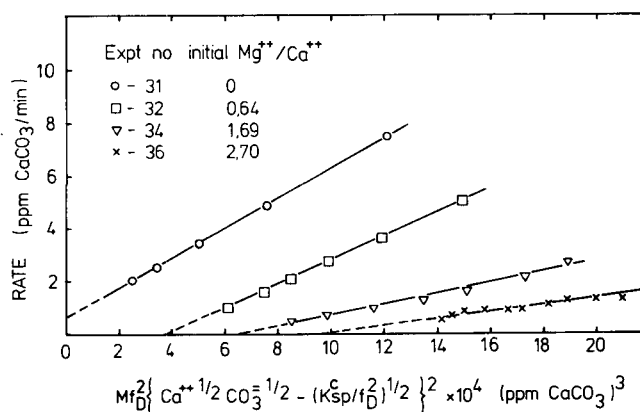


Figure 3
Plots of rate versus calcite supersaturation function do not pass through the origin

Plots are shown in Fig. 3 of the precipitation rate, $\delta\text{Ca}_T/\delta t$, versus supersaturation function, $Mf_D^2\{\text{Ca}^{++}\frac{1}{2}\text{CO}_3^{\frac{1}{2}} - K_{sp}^c\frac{1}{f_D}\}^2$, for a number of experiments in which the initial $(\text{Mg}^{++})/(\text{Ca}^{++})$ ratio varies from 0 to 2.84 using K_{sp}^c for pure calcite. From Fig. 3 the following points are evident:

- the plots are apparently straight lines
- the slope (i.e. the rate constant) decreases with increasing initial $(\text{Mg}^{++})/(\text{Ca}^{++})$ ratio, but remains constant in any particular experiment although the $(\text{Mg}^{++})/(\text{Ca}^{++})$ ratio increases.
- the plots do not pass through the origin – with increasing $(\text{Mg}^{++})/(\text{Ca}^{++})$ ratios plot intersections move away from the origin along the function axis.
- comparing experiments with and without Mg^{++} : where Mg^{++} is present the rate of precipitation is reduced at any particular supersaturation function value.

The observation that the plots do not pass through the origin implies that when the rate of precipitation is zero, the solution is still supersaturated with respect to calcite (because the function value is not zero). This would indicate that there is a change in the solubility product of the precipitant as implied in our hypothesis, that a magnesian calcite is being precipitated. If so, the precipitate should show the presence of magnesium ions. To verify this, a number of thoroughly washed samples of the precipitate were examined by X-ray analysis. These revealed the presence of Mg^{++} , up to approximately 5 percent of the CaCO_3 precipitated, and no trace of aragonite.

The calculations were repeated using the apparent solubility product, K_{spa} , which varies with the $(\text{Mg}^{++})/(\text{Ca}^{++})$ ratio in accordance with the observations of Winland (1969) and Plummer and Mackenzie (1974), see Eqs. (4 and 5).

Plots of the rate, $-\delta\text{Ca}_T/\delta t$, versus the modified supersaturation function, $Mf_D^2\{\text{Ca}^{++}\frac{1}{2}\text{CO}_3^{\frac{1}{2}} - (K_{spa}/f_D^2)\frac{1}{2}\}^2$ are shown in Fig. 4. Note that during precipitation a small fraction of magnesium is removed from the water together with the calcium. This change in magnesium is incorporated in the rate computations (see Appendix A) to estimate both the instantaneous value of K_{spa} using Eq. (5) and the mass of CaCO_3 removed as follows:

$$\Delta \text{Alkalinity} = (1 - x) \Delta\text{Ca}_T + x\Delta\text{Mg}_T \quad (22)$$

From Fig. 4 the plots are now curved but appear to pass through the origin. The fact that the plots pass through the origin would indicate that the solubility product does indeed increase as the $\text{Mg}^{++}/\text{Ca}^{++}$ ratio increases. The fact that the plots are curved would indicate that the rate constant, K , given by the slopes of the curves, is also influenced by the instantaneous $(\text{Mg}^{++})/(\text{Ca}^{++})$ ratio. From these curves it is difficult to identify the relationship between K and the $(\text{Mg}^{++})/(\text{Ca}^{++})$ ratio. A clearer understanding of the variation of K with $(\text{Mg}^{++})/(\text{Ca}^{++})$ can be obtained by making plots of the rate versus the supersaturation function for a constant $(\text{Mg}^{++})/(\text{Ca}^{++})$ ratio. To obtain such plots from the experimental data the following method was employed:

\log_e rate was plotted against $(\text{Mg}^{++})/(\text{Ca}^{++})$ ratio for a constant value of the supersaturation function. This was done as follows: Plots of the rate versus the supersaturation function

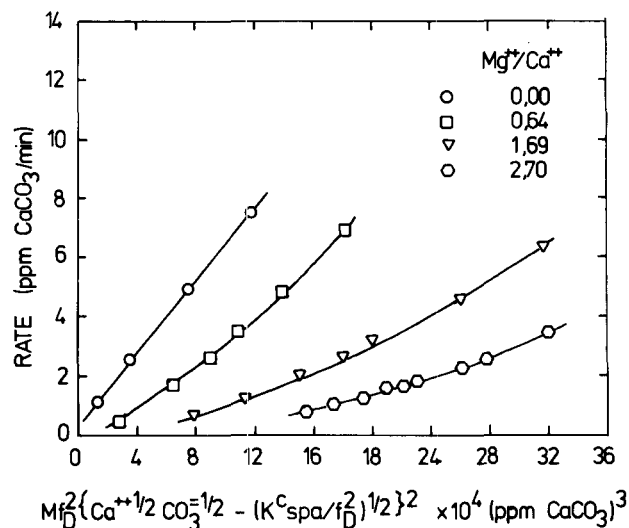


Figure 4
Plots of rate versus magnesian calcite supersaturation function, apparently pass through the origin but show curvature

are shown in Fig. 4. For particular supersaturation function value, corresponding values of the rate and $(\text{Mg}^{++})/(\text{Ca}^{++})$ were determined. This was done for each experiment. Using the values thus obtained, plots of \log_e rate versus $(\text{Mg}^{++})/(\text{Ca}^{++})$ were made for fixed supersaturation function values (15.10^4 , 20.10^4 , 25.10^4 , 30.10^4 , 35.10^4 and 40.10^4 (ppm as CaCO_3)³). The plots are shown in Fig. 5. It is evident that for each value of the supersaturation function, the rate of precipitation decreases as the $(\text{Mg}^{++})/(\text{Ca}^{++})$ increases, and appears to be of the form

$$\text{Rate} = \text{Ce}^{-k (\text{Mg}^{++})/(\text{Ca}^{++})} \quad (23)$$

where

$C, k = \text{constants.}$

A mean straight line is drawn through the data in each of the plots (see Fig. 5), and values of the rate of precipitation are read off for any particular $(\text{Mg}^{++})/(\text{Ca}^{++})$ ratio at a particular supersaturation function value. Selecting a particular $(\text{Mg}^{++})/(\text{Ca}^{++})$ ratio, say 2.0, rates are read off from each of the six plots giving six supersaturation function values corresponding to the rates. Using the values thus obtained, a plot of the rate versus the supersaturation function for $(\text{Mg}^{++})/(\text{Ca}^{++}) = 2.0$ is made, see Fig. 6. In the same fashion plots of the rate versus the supersaturation function are made at $(\text{Mg}^{++})/(\text{Ca}^{++})$ ratios of 0.0, 1.0, 3.0 and 4.0, see Fig. 6. The plots all appear to pass through the origin indicating that when precipitation ceases, the solution is saturated with respect to magnesian calcite. The slope K^c remains constant for a fixed $(\text{Mg}^{++})/(\text{Ca}^{++})$ ratio. The relationship between K^c and $(\text{Mg}^{++})/(\text{Ca}^{++})$ is shown in Fig. 7, i.e.

$$\log_e K^c = \log_e K_o^c - 0.564 (\text{Mg}^{++})/(\text{Ca}^{++}) \quad (24)$$

where

$K_o^c = \text{rate constant when no } \text{Mg}^{++} \text{ is present and equals } 5.7.10^{-6} \text{ (min. (ppm as } \text{CaCO}_3\text{)}^2)^{-1}$

Rearranging Eq. (24)

$$K^c = K_o^c e^{-0.564 (\text{Mg}^{++})/(\text{Ca}^{++})} \quad (25)$$

- (1) *Pseudomonas* C (Chalfun and Mateles, 1972; 1974)
- (2) *Methylobacterium methanolicum* (Dostálek *et al.*, 1972)
- (3) I.C.I. methanol bacterium *Pseudomonas* strain (McLennan *et al.*, 1973)
- (4) Mitsubishi Gas Chemical Company – *Pseudomonas* spp (Nagai, 1973)
- (5) *Pseudomonas* strain utilising methane and *Hyphomicrobium* strain utilising methanol (Wilkinson and Harrison, 1973)
- (6) Mixed culture of thermotolerant bacteria (Snedecor and Cooney, 1974)

The above strains have all been cultured aerobically. However, under anoxic conditions with methanol and nitrate it was found (Nurse, 1976) that the cells present belonged predominantly to the genus *Hyphomicrobium*. This result confirms the findings of two independent groups, each of which found that with a wide variety of inocula, anaerobic conditions with methanol as carbon and energy source result in rapid and specific enrichment for *Hyphomicrobium* spp (Sperl and Hoare, 1971; Attwood and Harder, 1972).

Although *Hyphomicrobium* spp have been of interest to researchers in carbon-one metabolism for a number of years there is little published information on the basic kinetic parameters and coefficients which characterise the group under aerobic and anaerobic conditions, especially with respect to continuous culture. Unfortunately, since denitrification can be performed by a wide variety of common facultative bacteria, it has always been concluded by workers in this field that little can be achieved from identification of species actively performing in their plants.

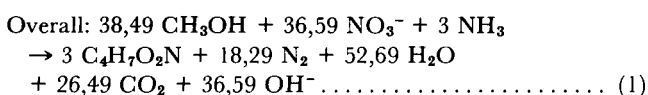
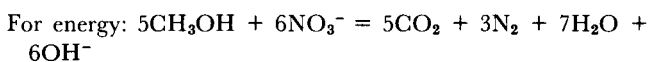
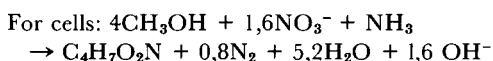
Investigations have therefore been undertaken not only to obtain quantitative growth parameters that may be used for design purposes to optimise a denitrification treatment, but also to characterise the bacteria which exist under the experimental conditions and to show how the inherent properties of the organisms limit a parameter.

A detailed review of the literature and the development of the biochemical reactions is given by Nurse (1977).

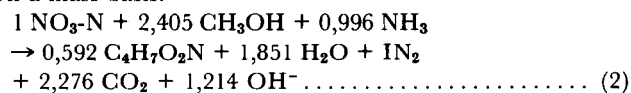
Nature of reactions

Based on the studies of Nurse (1977) and assuming a cell composition of $C_4H_7O_2N$, the following stoichiometric relations seem to describe the reactions:

In the presence of nitrate-N and ammonia-N



On a mass basis:

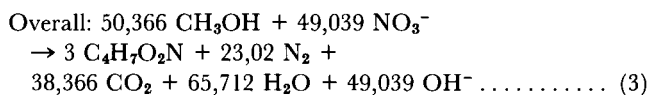
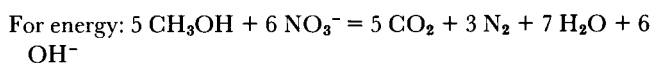
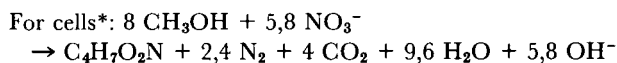


Hence $Y = 0,246$

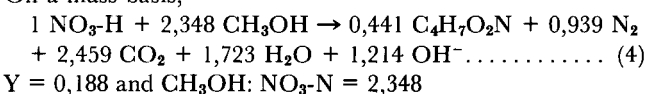
and $CH_3OH: NO_3-N = 2,405$

or $CH_3OH: \text{Total N} = 2,223$

In presence of nitrate-N only (NH_3-N absent)



On a mass basis,

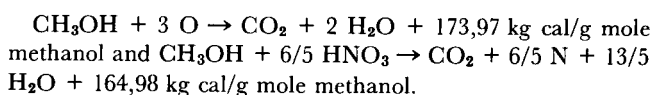


$Y = 0,188$ and $CH_3OH: NO_3-N = 2,348$

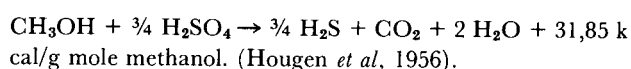
From an alcohol consumption point of view, it is better therefore to denitrify in the presence of ammonia-N, but in view of NH_3 toxicity to maintain an ammonia level in the feed which will match the assimilation requirement.

Energy release

The oxidation of methanol by oxygen and nitrate respectively results in the release of different amounts of energy:



Similarly, the oxidation of methanol by H_2SO_4 results in some energy release:



Although the difference in energy release is small when NO_3^- replaces O_2 as terminal electron acceptor, it is important to

*Though the cofactor and physiological electron acceptor for the enzyme methanol dehydrogenase (responsible for the oxidation of $CH_3OH \rightarrow HCHO$ and $HCHO \rightarrow HCOOH$ in *Hyphomicrobium* spp) remains unclear, it is assumed that they are reoxidised by the electron transport chains associated with the reduction of $NO_3^- \rightarrow N_2$. This assumption is based on the finding that CH_3OH consumed for energy purposes is recovered as CO_2 and that no intermediates accumulate. Furthermore, *Hyphomicrobium* spp lacks the capacity to ferment.

For the conversion of $NO_3^- \rightarrow NH_3$ for assimilatory purposes it has been assumed that the hydrogens required are only made available for this purpose from the oxidation of $HCOOH$ to CO_2 , the enzyme formate dehydrogenase in *Hyphomicrobium* spp has been shown to be NAD dependent. Hence chemically, the conversion of $NO_3^- \rightarrow NH_3$ may be represented by the following equation: $4CH_3OH + 4,2NO_3^- \rightarrow 4CO_2 + NH_3 + 1,6N_2 + 4,4H_2O + 4,2OH^-$

ensure that anoxic conditions are present since *Hyphomicrobium* spp, being facultative aerobes, will preferentially utilize O_2 instead of NO_3^- . Furthermore, the presence of NO_3^- is required to prevent formation of H_2S by the third reaction given above.

Production of alkaline conditions

Denitrification raises the pH of the substrate as shown in reactions (1) and (3).

By maintaining a maximum of CO_2 in the solution in the reactor, the acid requirement for OH^- neutralisation can be reduced, and in continuous stirred tank (CST) reactors this can be done effectively by circulating the off-gases and so also effecting agitation.

Toxic and inhibitory materials

Heavy metals in general exhibit toxicity but these are absent or present at very low levels only in the effluent under consideration. Ammonia, nitrite and sulphide are likely to occur in a reactor under specific conditions. The free species of these materials are generally considered to be toxic.

At any concentration the proportion of free (non-ionised) species is highly dependent on pH of the solution and operation of any reactor will be adversely affected unless adequate pH control is carried out. Figure 1 depicts the variation of ionisation of various species with pH. Without affecting bacterial action significantly by OH^- or H^+ , both ammonia and nitrous acid can be reduced by operation near pH 7. Unfortunately H_2S exists over a large pH range and control cannot be effected by pH control. On the other hand, provided NO_3^- is not reduced to zero, H_2S will not be generated from any SO_4^{2-}

in the reactor. Should such a situation arise where NO_3^- is taken to zero, and H_2S is generated, the reactor contents could be treated with a ferrous salt to remove the free H_2S as an 'insoluble' iron sulphide. This condition may arise when excess methanol is present in the reactor.

A denitrifying reactor should be run under methanol limited conditions for a reason other than possible H_2S formation, namely methanol inhibition. Methanol toxicity has been shown to exist for a number of methanol utilising bacteria (Nurse, 1977) and should not be allowed to occur in a plant designed on parameters obtained under methanol limited conditions since an inhibition term is warranted when present in excess.

Single step reaction

No significant nitrite production should occur in a well operated system and it is considered that nitrate conversion to nitrogen may be regarded as a single step reaction for design purposes. The following equations (Neytzel-de Wilde, 1975) were thus applied to the results given in this work.

With sufficient other nutrients present, the growth controlling substrate will be either methanol or nitrate. If nitrate were the growth limiting factor, the nitrate-N removal efficiency could be changed only by varying the sludge retention time (R_s). If methanol concentration controlled microbial growth, then the sludge retention time (R_s) would in addition determine the effluent COD.

The stoichiometric equations (2) and (4) show that a given quantity of methanol is required to remove a given quantity of NO_3^- . This amount of nitrate-N removed depends on the influent methanol concentration as well as the sludge retention time.

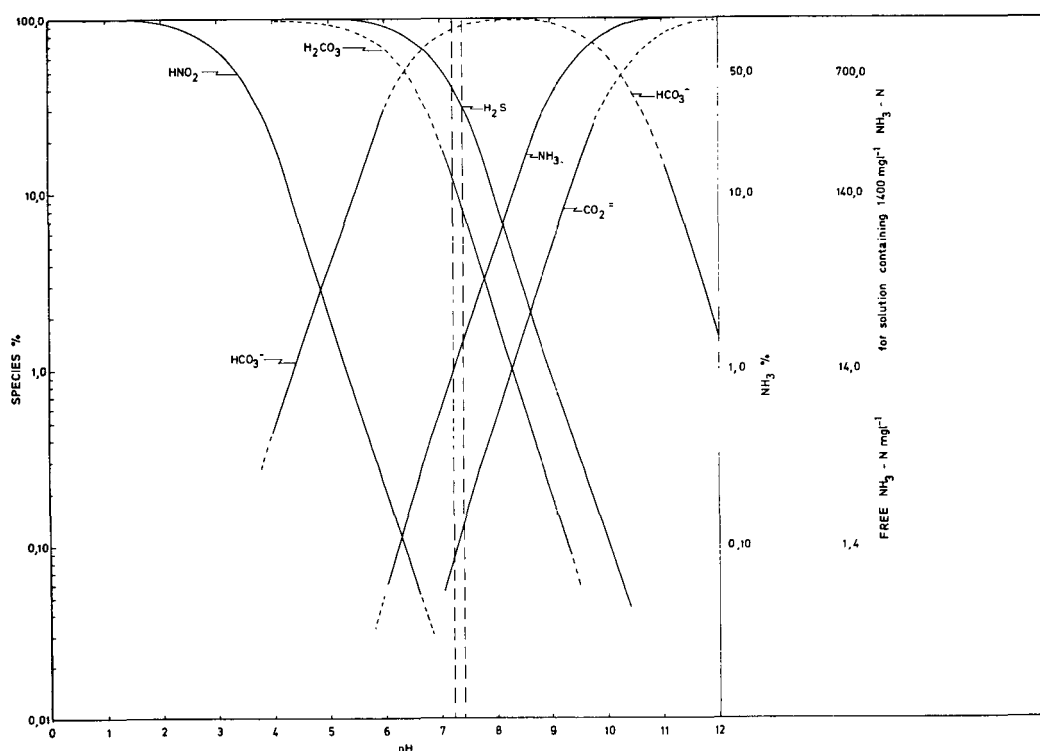


Figure 1
Variation of ionisation with pH

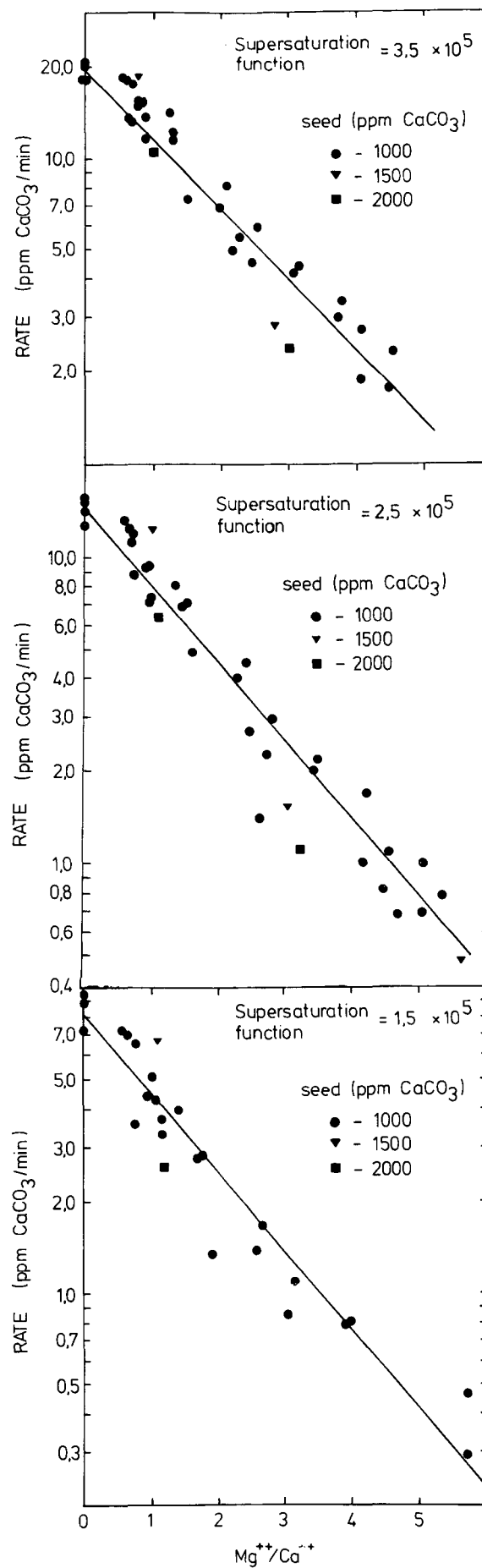
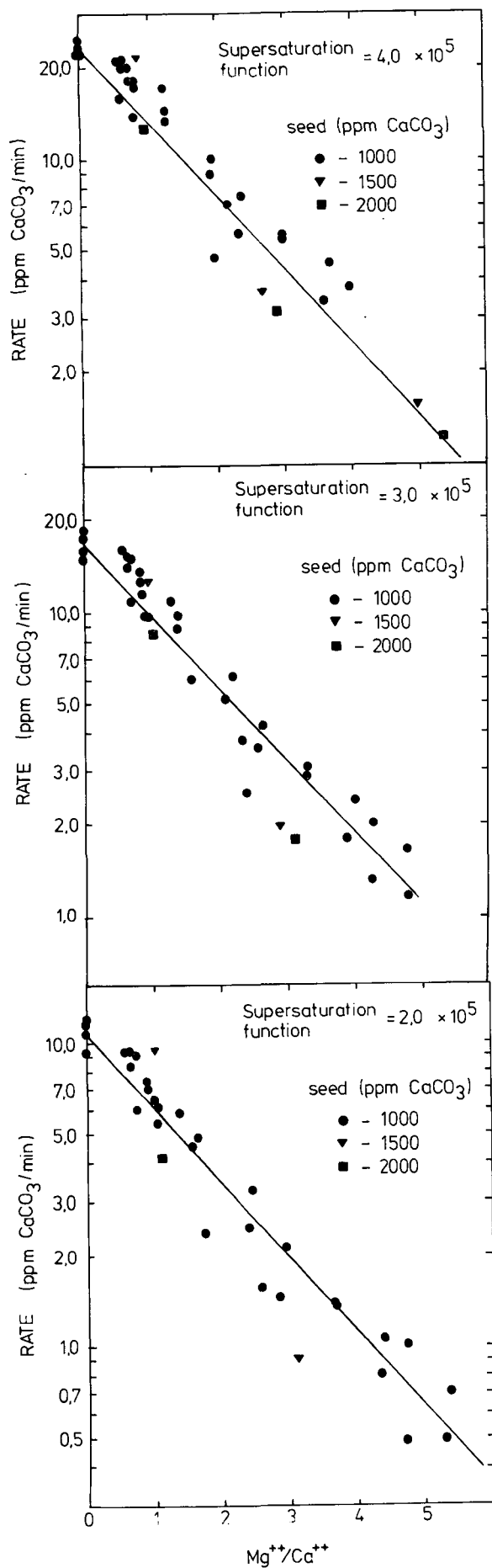


Figure 5
Plots of rate versus $(\text{Mg}^{++})/(\text{Ca}^{++})$ ratio for selected constant supersaturation function values

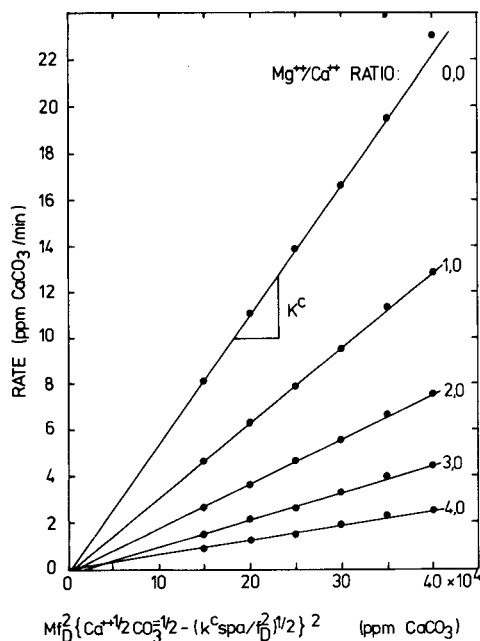


Figure 6
Plots of rate versus magnesian calcite supersaturation function for selected constant values of $(Mg^{++})/(Ca^{++})$ ratio

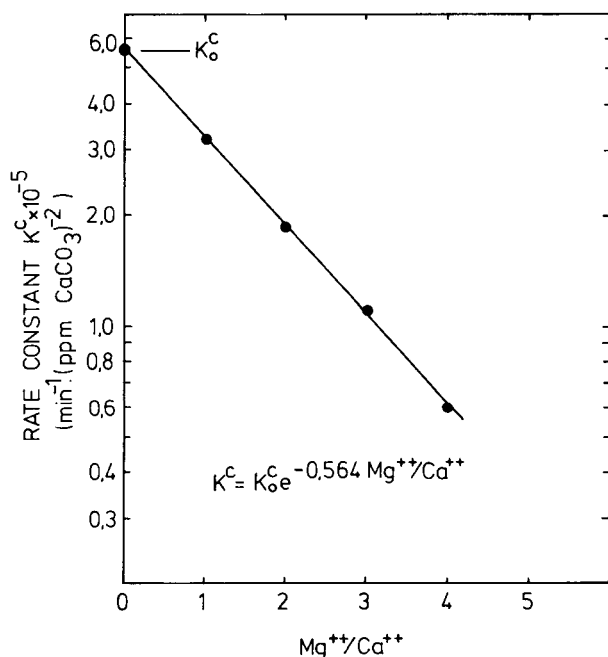


Figure 7
Precipitation rate constant for magnesian calcite versus $(Mg^{++})/(Ca^{++})$ ratio

The observation that the solubility product increases and the rate constant for precipitation decreases with increase in $(Mg^{++})/(Ca^{++})$ ratio in the aqueous phase explains the behaviour observed on full scale plants, i.e. (1) the final value of calcium in solution is greater than that predicted on the basis of calcite solubility and (2) the reaction time to near saturation is longer. These effects may be significant even when the ratio of $(Mg^{++})/(Ca^{++})$ in the raw water is 1/3 or less: As $CaCO_3$ is precipitated the magnesium concentration remains virtually unaffected so that the final $(Mg^{++})/(Ca^{++})$ ratio in the solution may attain high values of five or more. Thus with the low lime

system of calcium softening of hard waters containing both calcium and magnesium, it will not be possible to remove calcium to low concentrations. The more general practical implications are considered in a future paper.

Conclusions

1. When magnesium is present in the solution the Davies and Jones hypothesis still appears to be valid, but due regard must be taken of the influence of Mg^{++} on the crystallisation as follows: When magnesium is present in solution, Mg^{++} ions are incorporated into the crystal to form some type of magnesian calcite, the fraction of Mg^{++} incorporated depending on the $(Mg^{++})/(Ca^{++})$ ratio in the solution. The presence of Mg^{++} increases the solubility product and reduces the rate constant of precipitation, both being dependent on the particular magnesian calcite crystal type being deposited at the moment. The magnesian calcite crystal type is also a function of the $(Mg^{++})/(Ca^{++})$ ratio, hence both the solubility product, K_{spm} and the rate constant, K , are functions of the $(Mg^{++})/(Ca^{++})$ ratio. These effects are incorporated in the modified form of the rate equation, i.e.

$$-\delta[Ca_T]\delta t = KMf_D^2\{[Ca^{++}]^{\frac{1}{2}}[CO_3^{\frac{1}{2}}] - (K_{spa}/f_D^2)^{\frac{1}{2}}\}^2$$

where

K_{spa} = the apparent $CaCO_2$ solubility product and is calculated from the magnesian calcite solubility product, K_{spm} , as follows

$$K_{spa} = K_{spm} \{(Mg^{++})/(Ca^{++})\}^x \text{ and}$$

$$pK_{spm} = 8.40 - 1.744x \text{ (25°C) and}$$

$$x = 1/[1 + 50(Ca^{++})/(Mg^{++})]$$

where

x = the mole fraction of $MgCO_3$ in the magnesian calcite.

The rate constant for precipitation, K , varies with the $(Mg^{++})/(Ca^{++})$ ratio according to the relationship

$$K = K_o^C e^{-0.564(Mg^{++})/(Ca^{++})}$$

where

K_o^C = rate constant when no magnesium is present.

2. The fraction of magnesium in the crystal is small ranging from 0 to 5 percent of the total calcium deposited. Consequently during precipitation the $(Mg^{++})/(Ca^{++})$ ratio increases, thereby increasing the final solubility product and decreasing the rate of precipitation. The final concentration of $[Ca_T]$ is therefore governed by the final $(Mg^{++})/(Ca^{++})$ and $(Ca^{++})/(CO_3^{\frac{1}{2}})$ ratio, ionic strength and temperature.

3. With regard to the removal of calcium in full scale plants, when magnesium is present the reactor retention time must be longer to compensate for the slower rate of precipitation. In the final state the water will contain higher concentrations of calcium compared with an identical plant with identical concentrations of calcium and carbonates when magnesium is not present.

Acknowledgement

The authors gratefully acknowledge the financial support of the South African Council for Scientific and Industrial Research.

References

- BENJAMIN, L., LOEWENTHAL, R.E. and MARAIS, G.v R., (1976) The effect of magnesium ions on calcium carbonate precipitation kinetics, *Interim Report*, W/20, Dpet. of Civil Engineering, University of Cape Town.
- BERNER, R.A. (1975) The role of magnesium in the crystal growth of calcite and aragonite from sea water, *Geochemica et Cosmochimica* **39** 489.
- CHAVE, K.E., DEFFEYES, K.S., WEYL, P.K., GARRELS, R.M. and THOMPSON, M.E., (1962) Observations on the solubility of skeletal carbonates in aqueous solutions, *Science* **137** 33.
- DAVIES, C.W. and JONES, A.L., (1955) The precipitation of silver chloride from aqueous solutions, *Trans. Faraday Soc.* **51** 812.
- DAVIES, C.W. and NANCOLLAS, G.H., (1955) The precipitation of silver chloride from aqueous solutions – the influence of foreign ions, *Trans. Faraday Soc.* **51** 823.
- DE GROOT, K. and DUYVIS, E.M., (1966) Crystal form of precipitated calcium carbonate as influenced by adsorbed magnesium ions, *Nature* **212** 183.
- GARRELS, R.M. and CHRIST, C.L. (1965) *Solutions, Minerals and Equilibria*, Harper and Row, New York.
- HELGESON, H.C. (1969) Thermodynamics of hydrothermal systems at elevated temperatures and pressures, *Am. J. of Sci.* **267** 729.
- KRAUSKOPF, K.B. (1967) *Introduction to geochemistry*, McGraw Hill, New York, 721.
- LARSON, T.E., SOLLO, F.W. and MCGURK, F.F., (1973) *W.R.C. Research Report*, Water Research Centre, University of Illinois.
- LOEWENTHAL, R.E. and MARAIS, G.v R., (1976) Carbonate chemistry of aquatic systems, *Ann Arbor Science*, Michigan, 209.
- MCLEAN, A., (1976) Determination of ion pair constants in the carbonic system, *Progress Report to C.S.I.R., South Africa*.
- PLUMMER, L.N. and MACKENZIE, F.T. (1974) Predicting mineral solubility from rate data, *Am. J. Sci.* **274** 61.
- PYTKOWICZ, R.M. (1965) Rates of inorganic calcium carbonate nucleation, *J. Geol.* **73** 61.
- ROQUES, H. and GIROU, A., (1974) Kinetics of formation conditions of carbonate tartars, **8** 907.
- STUMM, W. and MORGAN, J.J. (1970) *Aquatic Chemistry*, New York, Wiley Interscience, 271.
- WIECHERS, H.N.S., STURROCK, P.L.K. and MARAIS, G.v.R. (1975) Calcium carbonate crystallization kinetics, *Water Research* **9** 835.
- STURROCK, P.L.K., BENJAMIN, L., LOEWENTHAL, R.E. and MARAIS, G.v. R. (1976) Calcium carbonate precipitation kinetics. Part 1. Pure system kinetics, *Water SA* **3** 101.
- WINLAND, H.D. (1969) Stability of calcium carbonate polymorphs in warm shallow sea water, *J. Sed. Petrol.* **39** 1579.

Appendix A

The procedure for calculating the parameters that influence the rate equation Eq. (20), is described below. The method utilizes the relationship between Alkalinity, Acidity and pH (Loewenthal and Marais, 1976) and is not restricted to any pH range.

The pH in a water containing only carbonic species and associated cations is governed by equilibria reactions between the carbonic species (H_2CO_3^* , and HCO_3^- and CO_3^{2-}) and water species (H^+ and OH^-). These equilibria are:

$$(\text{HCO}_3^-) (\text{H}^+)/(\text{H}_2\text{CO}_3^*) = K_1 \quad (\text{A1})$$

$$(\text{CO}_3^{2-}) (\text{H}^+)/(\text{HCO}_3^-) = K_2 \quad (\text{A2})$$

$$(\text{OH}^-) (\text{H}^+) = K_w \quad (\text{A3})$$

where

() indicate active concentrations

K_1 , K_2 and K_w = thermodynamic equilibrium constants.

If calcium, magnesium and sodium ions are in the water, ion pairing will occur between these cations and the anions CO_3^{2-} , HCO_3^- and OH^- . Equilibria equations for these ion pairing reactions are:

$$(\text{Ca}^{++}) (\text{CO}_3^{2-})/(\text{CaCO}_3^0) = K_{\text{CaCO}_3^0} \quad (\text{A4})$$

$$(\text{Ca}^{++}) (\text{HCO}_3^-)/(\text{CaHCO}_3^+) = K_{\text{CaHCO}_3^+} \quad (\text{A5})$$

$$(\text{Ca}^{++}) (\text{OH}^-)/(\text{CaOH}^+) = K_{\text{CaOH}^+} \quad (\text{A6})$$

$$(\text{Na}^+) (\text{CO}_3^{2-})/(\text{NaCO}_3^-) = K_{\text{NaCO}_3^-} \quad (\text{A7})$$

$$(\text{Na}^+) (\text{HCO}_3^-)/(\text{NaHCO}_3^0) = K_{\text{NaHCO}_3^0} \quad (\text{A8})$$

$$(\text{Mg}^{++}) (\text{CO}_3^{2-})/(\text{MgCO}_3^0) = K_{\text{MgCO}_3^0} \quad (\text{A9})$$

$$(\text{Mg}^{++}) (\text{HCO}_3^-)/(\text{MgHCO}_3^+) = K_{\text{MgHCO}_3^+} \quad (\text{A10})$$

$$(\text{Mg}^{++}) (\text{OH}^-)/(\text{MgOH}^+) = K_{\text{MgOH}^+} \quad (\text{A11})$$

For equilibrium the equations, Eqs. (A1 to A11) must be simultaneously satisfied. The following mass balance expressions must also be satisfied

$$[\text{Na}]_T = [\text{Na}^+] + [\text{NaHCO}_3^0] + [\text{NaCO}_3^-] \quad (\text{A12})$$

$$[\text{Ca}]_T = [\text{Ca}^{++}] + [\text{CaHCO}_3^+] + [\text{CaCO}_3^0] + [\text{CaOH}^+] \quad (\text{A13})$$

$$[\text{Mg}]_T = [\text{Mg}^{++}] + [\text{MgHCO}_3^+] + [\text{MgCO}_3^0] + [\text{MgOH}^+] \quad (\text{A14})$$

$$[\text{HCO}_3^-]_T = [\text{HCO}_3^-] + [\text{CaHCO}_3^+] + [\text{NaHCO}_3^0] + [\text{MgHCO}_3^+] \quad (\text{A15})$$

$$[\text{CO}_3^{2-}]_T = [\text{CO}_3^{2-}] + [\text{CaCO}_3^0] + [\text{NaCO}_3^-] + [\text{MgCO}_3^0] \quad (\text{A16})$$

$$[\text{OH}^-]_T = [\text{OH}^-] + [\text{CaOH}^+] + [\text{MgOH}^+] \quad (\text{A17})$$

$$C_T = [\text{HCO}_3^-]_T + [\text{CO}_3^{2-}]_T + [\text{H}_2\text{CO}_3^*]_T \quad (\text{A18})$$

where

[] indicates molar concentrations, and subscript T indicates the sum of free and ion paired species concentration.

Equations (A1 to A18) constitute a set of eighteen independent equations containing twenty-three unknown parameters: (H , OH_T , OH^- , CO_{3T} , CO_3^{2-} , HCO_{3T} , HCO_3^- , H_2CO_3^* , Ca_T , Ca^{++} , Mg_T , Mg^{++} , Na_T , Na^+ , CaHCO_3^+ , CaOH^+ , CaCO_3^0 , MgHCO_3^+ , MgOH^+ , MgCO_3^0 , NaHCO_3^0 , NaCO_3^- , and C_T , all in molar form).

Thus, to calculate all the unknown species concentrations at least five parameters must be measured. The parameters $[\text{Na}]_T$, $[\text{Ca}]_T$ and $[\text{Mg}]_T$ can be measured by standard chemical methods. By measuring pH, $[\text{H}^+]$ can be calculated from the equation

$$\text{pH} = \log \{f_m[\text{H}^+]\} \quad (\text{A19})$$

Equation (A19) increases the number of independent equations to nineteen and the number of unknowns to twenty four. Hence, as four parameters are already known, one more parameter still needs to be measured for all the species concentrations to be calculated. If a total inorganic carbon analyser is available, C_T can be measured and inserted in Eq. (A18). If not, the equation for C_T must be replaced by an equation for some other measurable parameter which is expressed in terms of the basic unknowns. Alternatives to Eq. (A18) can be Alkalinity or Acidity. These are defined as follows:

$$\text{Alkalinity} = 2[\text{CO}_3^{2-}]_T + [\text{HCO}_3^-]_T + [\text{OH}^-]_T - [\text{H}^+] \quad (\text{A20})$$

$$\text{Acidity} = 2[\text{H}_2\text{CO}_3^*] + [\text{HCO}_3^-]_T + [\text{H}^+] - [\text{OH}^-]_T \quad (\text{A21})$$

where

Alkalinity is defined as moles of H^+ to change the pH of a water to that of an equivalent carbonic acid solution.

Acidity is defined as moles of OH^- to change the pH of a water to that of an equivalent carbonate solution.

In practice Alkalinity is easily estimated by titration as the carbonic acid end point is in a region of low buffer capacity. In contrast, Acidity is difficult to measure accurately by titration as the carbonate end point is in a region of high buffer capacity (Loewenthal and Marais, 1976). Nevertheless, Acidity is an important parameter for the reason that as calcite or magnesian calcite is precipitated it remains constant.

From the discussion above it is evident that by measuring $[\text{Na}]_T$, $[\text{Ca}]_T$, $[\text{Mg}]_T$, pH and Alkalinity, and using the independent Eqs. (A1 to A20), all species in the aqueous phase can be calculated. This will be true whether the water is undersaturated, saturated or supersaturated with respect to CaCO_3 provided neither dissolution nor precipitation of CaCO_3 occurs. When precipitation occurs calcium and carbonate are removed from solution in equimolar masses. This causes the Alkalinity to decrease (see Eq. A21) but the Acidity to remain constant (see Eq. A21). Hence the pH will change. By measuring the pH change it is therefore possible to calculate the Alkalinity change and hence the CaCO_3 precipitated.

In the method of solution described below, to initiate the solution theoretically only the initial pH and initial Alkalinity need be measured and thereafter as CaCO_3 precipitation proceeds only pH needs to be measured for an additional condition applies i.e. the Acidity remains constant during precipitation and equals the initial value.

Initial Alkalinity and Acidity were determined as follows: Solutions of NaHCO_3 and NaOH were standardised against a strong acid of known concentration. The standardised solutions of NaHCO_3 and NaOH were then used as the source of Alkalinity and Acidity for a particular test, thus

$$\text{Initial Alkalinity} = [\text{NaHCO}_3]_{\text{added}} + [\text{NaOH}]_{\text{added}}$$

$$\text{Initial Acidity} = [\text{NaHCO}_3]_{\text{added}} - [\text{NaOH}]_{\text{added}}$$

Initial pH was measured using a glass electrode.

However, CO_2 exchange between the solution and atmosphere may occur during the experimental preparation. From Eq. (A21) such CO_2 exchange would alter the initial Acidity (estimated from the known masses of standard solutions used); from Eq. (A20) the Alkalinity would not be affected. Thus the best estimate of initial Acidity is calculated from the initial imposed Alkalinity and the observed initial pH using Eqs. (A1 to A18). Usually the Acidity based on the measured pH was about 2 ppm as CaCO_3 greater than the observed Acidity. This theoretical check was carried out for each experiment as follows: Using the initial Alkalinity and Acidity values (based on the masses of stand solutions used) a theoretical value of initial pH was calculated using Eqs. (A1 to A18) and compared with the initial observed pH. If these pH values were different (inevitably the observed pH was too low), the Acidity was adjusted (decreased by about 2 ppm as CaCO_3) and the pH

recalculated. This corrected value of the Acidity, in nearly all cases, resulted in exact correspondence between calculated and observed pH.

Determination of initial acidity from known alkalinity and pH

1. Calculate an initial approximate value for ionic strength, μ , from the mass concentrations of NaOH , NaHCO_3 , CaCl_2 and MgCl_2 used in an experiment.
2. Using the extended Debye Hückel equation calculate the activity coefficients for each of the charged species from the value of μ above. (The ionic radius for monovalent hydrated ion pairs was assumed equal to that for HCO_3^- .)
3. Calculate activity coefficients for neutral species from the relationship $-\log_{10} f_N = k_s \mu$ where
 f_N = activity coefficient for neutral species
 k_s = salting out coefficient for neutral species in water.
4. Calculate thermodynamic equilibrium constants at the experimental temperature from the enthalpy and entropy for the reaction using the equation proposed by Helgeson (1969).
5. Adjust equilibrium constants for ionic strength effects to give K' .
6. Calculate $[\text{H}^+]$ from the measured pH and the approximate value for the activity coefficient, f_H , determined in step (2), i.e. $[\text{H}^+] = (10^{-\text{pH}})/f_H$.
7. Calculate an approximate initial value for $[\text{HCO}_3^-]$ from measured Alkalinity and pH assuming no ion pairing, i.e. $[\text{HCO}_3^-] = [\text{Alk} - K_1'/([\text{H}^+] + [\text{H}^+])]/(1 + 2K_2'/[\text{H}^+])$.
8. Calculate values for $[\text{H}_2\text{CO}_3^*]$, $[\text{CO}_3^{2-}]$ and $[\text{OH}^-]$ from equilibrium equations, Eqs. (A1 to A3), and the assumed values for $[\text{H}^+]$ and $[\text{HCO}_3^-]$, i.e.
 $[\text{H}_2\text{CO}_3^*] = [\text{H}^+][\text{HCO}_3^-]/K_1'$ and $[\text{CO}_3^{2-}] = K_2'[\text{HCO}_3^-]/[\text{H}^+]$
9. Calculate ion paired species $[\text{NaCO}_3^-]$, $[\text{NaHCO}_3^0]$, $[\text{MgCO}_3^0]$, $[\text{MgHCO}_3^+]$, $[\text{MgOH}^+]$, $[\text{CaCO}_3^0]$, $[\text{CaHCO}_3^+]$ and $[\text{CaOH}^+]$ from equilibrium equations, Eqs. (A4 to A11). (In the first iteration the species concentrations $[\text{Ca}^{++}]$, $[\text{Mg}^{++}]$ and $[\text{Na}^+]$ are assumed equal to the total analytical concentrations of these species $[\text{Ca}]_T$, $[\text{Mg}]_T$ and $[\text{Na}]_T$.
 In all subsequent iterations the values for $[\text{Ca}^{++}]$, $[\text{Mg}^{++}]$ and $[\text{Na}^+]$ used are those calculations from the previous iteration, i.e. those values calculated in step 10.
10. Calculate adjusted values for $[\text{Na}^+]$, $[\text{Ca}^{++}]$ and $[\text{Mg}^{++}]$, e.g.
 $[\text{Na}^+] = [\text{Na}]_T - [\text{NaHCO}_3^0] - [\text{NaCO}_3^-]$
11. (i) Calculate values for Alkalinity and Acidity from the values for individual species determined above using Eqs. (A20 and A21), i.e. $\text{Alk (calculated)} = 2([\text{CO}_3^{2-}] + [\text{NaCO}_3^-] + [\text{CaCO}_3^0] + [\text{MgCO}_3^0]) + ([\text{HCO}_3^-] + [\text{NaHCO}_3^0] + [\text{CaHCO}_3^+] + [\text{MgHCO}_3^+] + [\text{OH}^-] + [\text{CaOH}^+] + [\text{MgOH}^+]) - [\text{H}^+]$
 $\text{Acidity (calculated)} = 2[\text{H}_2\text{CO}_3^*] + ([\text{NCO}_3^-] + [\text{NaHCO}_3^0] + [\text{CaHCO}_3^+] + [\text{MgHCO}_3^+] + [\text{H}^+] - [\text{OH}^-] + [\text{CaOH}^+] + [\text{MgOH}^+])$

- (ii) Calculate an adjusted value for ionic strength, from the individual species concentrations determined in steps 8 and 9.
 - (iii) Recalculate the activity coefficients, and adjust the equilibrium constants accordingly.
 - (iv) Recalculate $[H^+]$ from the measured pH and adjusted activity coefficient f_H .
12. Steps 7 to 11 are then reiterated until the calculated value for Alkalinity remains constant.
 13. Compare the calculated value for Alkalinity, Alk (calculated) with the known initial Alkalinity.
 14. Steps 8 to 13 are repeated with an adjusted value for $[HCO_3^-]$ until the calculated value for Alkalinity agrees with the true Alkalinity to within 10^{-7} moles/l. When this condition is satisfied Acidity is given by Acidity value calculated in step 11 (1). This calculated value usually will be $\pm 4 \cdot 10^{-6}$ moles/l greater than the Acidity value based on mass of chemicals used in solution and is due to CO_2 contamination. The calculated Acidity value is now assumed constant for the remaining calculations in the particular experiment.

Determination of alkalinity from known pH and acidity

During a precipitation experiment pH is monitored with time. Alkalinity values corresponding to the observed pH values are determined using the Acidity value calculated above (which remains constant with precipitation) and the observed pH

values. The method is essentially the same as that outlined above except that a known constant value for Acidity now replaces the previously known Alkalinity value in steps 7, 13 and 14. Precipitation rate computations are then executed in the following steps:

15. Calculate Alkalinity values corresponding to successive observed pH values over the time increment Δt_1 . The Alkalinity change equals the mass concentration of calcium and magnesium precipitated in the magnesium calcite during time interval Δt_1 :

$$\Delta \text{Alkalinity} = \Delta [Ca]_T + \Delta [Mg]_T$$

The fraction of magnesium precipitated, $\Delta [Mg]_T$, depends on the order of the magnesium calcite precipitating. This in turn, depends on the $(Mg^{++})/(Ca^{++})$ ratio in the aqueous phase (a value which is initially known), i.e. from Eq. (9):

$$x = 1 / \{1 + 50,0 (Ca^{++}) / (Mg^{++})\}$$

where

x is the instantaneous mole fraction of magnesium in the precipitate.

Thus

$$\Delta [Mg]_T = x \Delta \text{Alk}$$

$$\Delta [Ca]_T = (1 - x) \Delta \text{Alk}$$

16. The value for $[Ca]_T$ and $[Mg]_T$ are then adjusted according to (15) above. Steps 1 to 15 are then repeated for the following pH value observed after time interval Δt_2 .